MNRAS 000, 1–5 (2018) Preprint 8 June 2019 Compiled using MNRAS LATEX style file v3.0

Dramatic spectral transition of X-ray pulsar GX 304−1 in low luminous state

Sergey S. Tsygankov,[1,2]⋆ Alicia Rouco Escorial,[3] Valery Suleimanov,[4,5,2] Alexander A. Mushtukov,[6,2,3] Victor Doroshenko,[4] Alexander Lutovinov,[2] Rudy Wijnands[3] and Juri Poutanen[1,2]

[1] *Department of Physics and Astronomy, FI-20014 University of Turku, Finland*
[2] *Space Research Institute of the Russian Academy of Sciences, Profsoyuznaya Str. 84/32, Moscow 117997, Russia*
[3] *Anton Pannekoek Institute of Astronomy, University of Amsterdam, Science Park 904, 1098 XH Amsterdam, The Netherlands*
[4] *Institut für Astronomie und Astrophysik, Universität Tübingen, Sand 1, D-72076 Tübingen, Germany*
[5] *Kazan (Volga region) Federal University, Kremlevskaya str. 18, 420008 Kazan, Russia*
[6] *Leiden Observatory, Leiden University, NL-2300RA Leiden, the Netherlands*

Accepted XXX. Received YYY; in original form ZZZ

ABSTRACT

We report on the discovery of a dramatic change in the energy spectrum of the X-ray pulsar GX 304−1 appearing at low luminosity. Particularly, we found that the cutoff power-law spectrum typical for accreting pulsars, including GX 304−1 at higher luminosities of $L_{\rm X} \sim 10^{36} - 10^{37}$ erg s^{-1}, transformed at lower luminosity of $L_{\rm X} \sim 10^{34}$ erg s^{-1} to a two-component spectrum peaking around 5 and 40 keV. We suggest that the observed transition corresponds to a change of the dominant mechanism responsible for the deceleration of the accretion flow. We argue that the accretion flow energy at low accretion rates is released in the atmosphere of the neutron star, and the low-energy component in the source spectrum corresponds to the thermal emission of the optically thick, heated atmospheric layers. We suggest that the high-energy component can be associated with thermally broadened cyclotron emission of the upper atmospheric layers overheated to $kT \sim 10 - 100$ keV. Alternative scenarios are also discussed.

Key words: accretion, accretion discs – pulsars: general – scattering – stars: magnetic field – stars: neutron – X-rays: binaries

1 INTRODUCTION

Spectral energy distribution of astrophysical objects reflects physical processes responsible for the observed emission. Extreme conditions in the vicinity of highly magnetized neutron stars (NS), X-ray pulsars (XRPs), result in a very complex interplay between various physical and geometrical effects happening in the emission regions. As a consequence, no physically motivated spectral model able to describe spectra of various XRPs at different luminosities emerged so far. Moreover, the existing models focus on the description of X-ray spectrum at high luminosities (see e.g. Becker & Wolff 2007; Farinelli et al. 2016) as no high-quality observations at low luminosities were available until recently. From observational point of view, spectra of all bright XRPs are quite similar, and can be roughly described with a cutoff power-law type continuum. We note, however, that there is at least one exception: a low-luminosity XRP X Persei.

The spectrum of this persistent Be X-ray binary (XRB) deviates significantly from the standard picture and exhibits two distinct humps with maxima around 10 and 60 keV. Several interpretations have been suggested to describe the observed spectrum. Di Salvo et al. (1998) proposed the continuum model consisting of two cutoff power-law components. The soft component was attributed to the partially thermalized emission from the NS atmosphere, whereas the hard component was suggested to be associated to the optically thin cyclotron emission in a strong magnetic field. Alternative interpretation was proposed by Doroshenko et al. (2012), who associated the two spectral components with thermal and bulk Comptonization in the vicinity of the NS. Finally, the source spectrum can be described with a single continuum component, for example, in the form of a power law modified by the high-energy cutoff, which is typical for bright XRPs. In this case, however, inclusion of a deep broad

⋆ E-mail: sergey.tsygankov@utu.fi

absorption feature at ~ 30 keV is required (cyclotron resonant scattering feature, CRSF; see e.g. Coburn et al. 2001; Lutovinov et al. 2012).

The main difference between the X Persei and others XRPs observed in broad energy band is that it has a significantly lower luminosity of a few times 10^{34} erg s^{-1}. Unfortunately, X Persei is a persistent source with insignificant variations in the mass accretion rate, so it was not possible to observe this source also at higher luminosities, and verify whether its spectrum at much higher accretion rates is more similar to that of other XRPs. On the other hand, observations of more distant sources at comparably low luminosity levels were not possible until recently, thus their behaviour at low accretion rates remained largely unexplored.

The situation has changed, however, with the launch of *NuSTAR* observatory (Harrison et al. 2013). In particular, detailed investigations of transient systems with Be companions (Be/XRP) known to exhibit giant outbursts covering luminosity range of up to 5 orders of magnitude (see e.g. Reig 2011) became possible.

In this work we present results of the spectral analysis of the X-ray emission from one of the most suitable for such research transient Be/XRP GX 304−1 observed with *NuSTAR* at a luminosity around 10^{34} erg s^{-1}, the lowest mass accretion rate ever observed for this source in a broad energy band. The source exhibits regular Type I outbursts almost every periastron passage (Kühnel et al. 2017), covering broad range of mass accretion rates. GX 304−1 has a relatively long pulse period of ~ 272 s (McClintock et al. 1977) and orbital period of ~ 132.5 d (Priedhorsky & Terrell 1983). The magnetic field of the NS in the system is known from the CRSF energy of ~ 54 keV (Yamamoto et al. 2011). Note that the CRSF energy also exhibits clear positive correlation with the source luminosity (Klochkov et al. 2012). The distance to the source is now known with high accuracy thanks to the *Gaia* results ($d = 2.01 \pm 0.15$ kpc, Treuz et al. 2018).

2 DATA ANALYSIS AND RESULTS

The source was observed with *NuSTAR* on 2018 June 3 (ObsID 90401326002; MJD 58272-58273). The raw data were processed following the standard data reduction procedures described in the *NuSTAR* user guide, and using the standard *NuSTAR* Data Analysis Software (NUSTARDAS) v1.6.0 provided under HEASOFT v6.24 with the CALDB version 20180814. The source and background spectra were extracted from the circular regions with radius of 60″ using the NUPRODUCTS routine. The background was extracted from a source-free region in the corner of the field of view. Total exposure time of the analyzed observation is 58 ks.

To expand our spectral analysis to lower energies, we used the data from the XRT telescope (Burrows et al. 2005) on-board the *Neil Gehrels Swift Observatory* (Gehrels et al. 2004) obtained simultaneously with *NuSTAR* (ObsID 00088780001). Observation was performed in Photon Counting (PC) mode with total exposure of 2 ks. Spectrum extraction was done using the online tools (Evans et al. 2009)[1] provided by the UK Swift Science Data Centre.

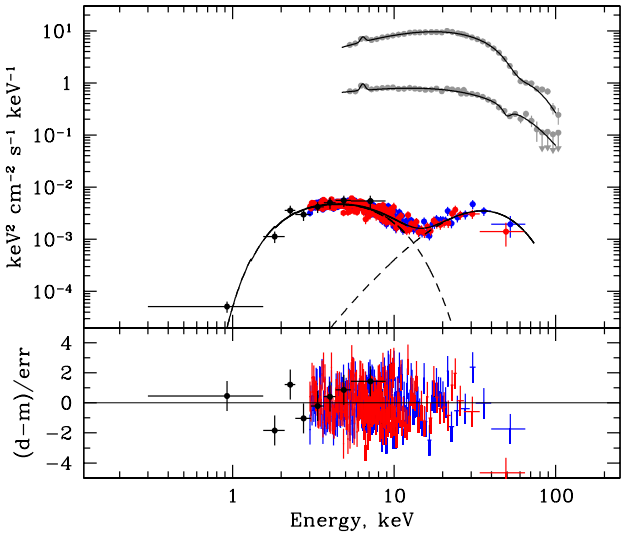

Figure 1. Spectra of GX 304−1 in different luminosity states in EF_E representation. The source luminosity varies by more than three orders of magnitude, from 2.2×10^{37} erg s^{-1} and 0.2×10^{37} erg s^{-1} for the two top spectra down to $\sim 10^{34}$ erg s^{-1} for the bottom one. Spectra in the bright states, shown with grey circles, are taken from Mushtukov et al. (2015b). The black, red and blue crosses correspond to the *Swift*/XRT and *NuSTAR* FPMA and FPMB data in the low state of GX 304−1, respectively. The solid line represents the best-fitting model consisting of two COMPTT components shown with dashed lines. The corresponding residuals are presented at the lower panel.

To fit the spectra in the XSPEC package we binned the spectra to have at least 1 count per energy bin and fitted them using W-statistic (Wachter et al. 1979).[2] The data from *Swift*/XRT and *NuSTAR* were used in the 0.3–10 keV and 3–79 keV bands, respectively.

The broadband spectrum of the source as observed by *NuSTAR* and *Swift*/XRT is shown in Fig. 1 along with two *INTEGRAL* spectra obtained at much higher luminosities of 2.2×10^{37} and 0.2×10^{37} erg s^{-1}(Mushtukov et al. 2015b). The peculiar double hump shape of the spectrum in the low state is immediately apparent. The observed flux implies that the source had luminosity around 10^{34} erg s^{-1}. Such luminosity is in line with the expected transition of the source to the state of stable low level accretion (Tsygankov et al. 2017b,a) rather than propeller regime (Illarionov & Sunyaev 1975) given the long spin period of the pulsar.

In the EF_E representation two humps with maxima around 5 and 40 keV have similar fluxes. Spectra in the bright states were fitted with the standard for XRPs power-law model modified with the high energy cutoff and a cyclotron absorption line at ~ 60 and ~ 50 keV for observations with $L = 2.2 \times 10^{37}$ and $L = 0.2 \times 10^{37}$ erg s^{-1}, respectively (Mushtukov et al. 2015b).

To fit the low-state spectrum we explored several models representing different combinations of physically moti-

[1] http://www.swift.ac.uk/user_objects/

[2] see XSPEC manual at https://heasarc.gsfc.nasa.gov/xanadu/xspec/manual/XSappendixStatistics.html

Table 1. Best-fitting results for the GX 304−1 broadband spectrum obtained with *NuSTAR*+*Swift*/XRT.

Parameter[a]	Low-energy part	High-energy part
compTT+compTT		
T_0, keV	0.46 ± 0.07	
kT_p, keV	$1.72^{+0.05}_{-0.08}$	$8.7^{+0.9}_{-0.4}$
τ_p	$8.4^{+1.3}_{-0.9}$	$\gtrsim 10$
F_X, 10^{-12} erg s^{-1} cm^{-2}	$13.3^{+0.3}_{-0.6}$	$7.2^{+1.0}_{-0.5}$
C-statistic (d.o.f.)	1813.3 (1875)	
compTT+gau		
T_0, keV	0.45 ± 0.07	
kT_p, keV	$1.72^{+0.08}_{-0.07}$	
τ_p	8.3 ± 0.5	
F_X, 10^{-12} erg s^{-1} cm^{-2}	$13.2^{+0.2}_{-0.3}$	
E_{gau}, keV		18^{+3}_{-5}
σ_{gau}, keV		16^{+3}_{-2}
F_X, 10^{-12} erg s^{-1} cm^{-2}		$6.6^{+0.7}_{-0.5}$
C-statistic (d.o.f.)	1810.3 (1875)	
CompTB		
kT_s, keV	$2.1^{+0.3}_{-0.2}$	
α	$0.3^{+0.1}_{-0.2}$	
γ	1.3 ± 0.2	
δ	$6.7^{+6.8}_{-4.9}$	
kT_e, keV	$3.4^{+2.5}_{-1.3}$	
log A	$-1.1^{+0.1}_{-0.4}$	
F_X, 10^{-12} erg s^{-1} cm^{-2}	$19.6^{+0.7}_{-0.5}$	
C-statistic (d.o.f.)	1815.6 (1877)	
compTT+Gabs		
T_0, keV	0.63 ± 0.04	
kT_p, keV	15 ± 6	
τ_p	$1.6^{+0.9}_{-1.5}$	
E_{gabs}, keV	14.9 ± 0.3	
σ_{gabs}, keV	$4.9^{+0.6}_{-0.5}$	
Depth$_{gabs}$	$13.3^{+3.5}_{-2.4}$	
F_X, 10^{-12} erg s^{-1} cm^{-2}	$25.7^{+1.8}_{-1.1}$	
C-statistic (d.o.f.)	1826.4 (1877)	

[a] Here kT_p, τ_p and T_0 are the plasma temperature, plasma optical depth, temperature of the seed photons for the compTT model. Fluxes are given for each spectral component in units of 10^{-12} erg s^{-1} cm^{-2} in the broad energy range of 0.5–100 keV. The hydrogen column density is fixed at the Galactic value in the source direction $N_H = 1.1 \times 10^{22}$ cm^{-2}. Description of parameters for the CompTB model can be found in Farinelli et al. (2008).

vated and phenomenological components. Particularly, to model the second hump in the spectrum as a separate emission component, we used (i) a combination of two Comptonization components (compTT+compTT model in xspec, Titarchuk 1994); (ii) a combination of Comptonization for the low-energy hump and an emission line with Gaussian profile for the high-energy one (compTT+Gau model in xspec); (iii) thermal and bulk Comptonization of a seed blackbody-like spectrum (CompTB model; Farinelli et al. 2008). Alternatively, the spectrum can be described with a single-component continuum modified by an absorption feature around 15 keV. In particular, we used compTT+Gabs combination. For all models we also included phabs component to take into account for interstellar photoelectric absorption at low energies. Because neither strong absorption was ever reported for this source, nor was required by our fit, we fixed the equivalent absorption column N_H at 1.1×10^{22} cm^{-2}, the Galactic value in this direction (Kalberla et al. 2005). To account for minor differences in the absolute flux calibration of the FPMA and FMPB instruments on-board *NuSTAR* and *Swift*/XRT telescope, the normalization factors were added to the separate data groups. As a result fluxes from FPMA and FMPB instruments match to within 2–3 per cent, whereas XRT normalization is about 1.3 times lower due to the fact that *NuSTAR* and *Swift* observations are not strictly simultaneous. In Fig. 1 the fit with two Comptonization components is shown with the corresponding residuals.

The fit results are presented in Table 1 and can be summarized as follows: (i) the spectrum can be fitted equally well with all four sets of models; (ii) in the case of two separate spectral components, the flux in the high-energy part is about half of the low-energy one; (iii) in the case of two Comptonization components, the plasma temperature of the high-energy component is about 5 times the low-energy one.

3 DISCUSSION

The spectrum of GX 304−1 in the low-luminosity state resembles the spectrum of another Be/XRP X Persei obtained at only slightly higher luminosity, $L_X \sim 8 \times 10^{34}$ erg s^{-1} (see Fig. 2). Both sources exhibit double-hump spectra with components peaking at energies separated by a factor of about 5–10. This similarity suggests that physical processes responsible for the spectrum formation at low mass accretion rates are also similar. In this section we discuss the possible nature of the emission from GX 304−1 in the low state and the reasons for the observed abrupt changes of the source spectrum. We note that similar mechanisms of spectral formation must be relevant also for other pulsars accreting at low rates including, but not limited to X Persei.

3.1 Cyclotron line

As already mentioned, a cyclotron line is observed in the spectrum of GX 304−1 at high luminosities (Walter et al. 2015). Moreover, a positive correlation of the line energy with the luminosity has been reported (Klochkov et al. 2012). Particularly, the energy was found to decrease from ~ 60 keV at luminosity of $L = 2.2 \times 10^{37}$ erg s^{-1} to ~ 50 keV at ten times lower luminosity (Mushtukov et al. 2015b). This behaviour was confirmed with the detailed analysis of the *RXTE* data (Rothschild et al. 2017). Therefore, one may argue that observed two component spectrum of the source is mimicked by an absorption feature at ~ 15 keV between two humps in the source spectrum, which is the cyclotron

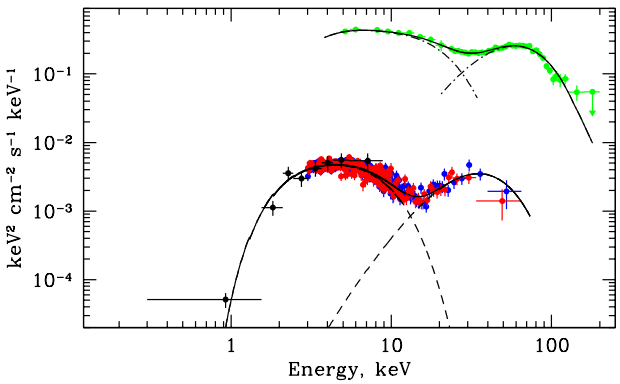

Figure 2. Spectra of X Persei as seen by the *INTEGRAL* observatory (green points) along with the best-fitting model consisting of two Comptonization components (see Doroshenko et al. 2012) and GX 304−1 fitted with the same model (see Fig. 1). Separate model components (COMPTT in XSPEC) are shown with dashed and dash-dotted lines for GX 304−1 and X Persei, respectively.

line shifted from the original ~ 60 keV due to substantially lower mass accretion rate.

The extrapolation of the observed correlation to low fluxes implies, however, significantly higher energy $E_{\rm cyc} \approx 30$ keV. Moreover, such a large decrease appears to be unrealistic in the context of the two models proposed so far to explain the observed correlation of line energy with flux. The first possibility is that the observed correlation is associated with the Doppler effect in the accretion flow (Mushtukov et al. 2015b). Indeed, the accretion flow, where the CRSF forms, is decelerated by radiative pressure, which is more efficient at higher luminosities. As a consequence, the flow velocity is lower for higher accretion rates, and the CRSF appears to be less red-shifted (i.e. at higher energies) for an external observer. In this model, the maximal relative shift is limited to ~ 0.5 by the maximal (free-fall) flow velocity. Because the highest observed line energy is ~ 60 keV, the lower possible energy in this scenario is ~ 30 keV, i.e. significantly higher than ~ 15 keV required to explain the observed spectrum of GX 304−1 in the low state with a single component continuum modified by an absorption feature.

The second model associates shifts of the CRSF energy with changes of the height of a collisionless shock above the NS polar cap (Rothschild et al. 2017). To explain the decrease from ~ 60 to 15 keV, the height of the line forming region must thus increase by half a NS radius R in this scenario. The geometric dilution of radiation is very significant at such height, resulting in only tiny part of the continuum photons from the hot polar cap to be scattered there. We conclude, therefore, that the description of the observed low luminosity spectrum of GX 304−1 with a single continuum component with a CRSF at ~ 15 keV is implausible also in this model.

3.2 Nature of the high-energy component

The conclusion above implies that the two humps in X-ray spectrum of the source are likely indeed two separate components, so we need to understand their origin. The soft blackbody-like component with a typical temperature of $kT \leq 2$ keV can be explained as radiation from hotspots at the NS surface heated up by the accretion process. However, the origin of the second component, which can also be fitted by a blackbody with the temperature $kT \approx 9$ keV or a broad Gaussian emission line (see Table 1) is much less clear.

First of all, similarly to X Persei, the spectrum can be formally described by the model of bulk Comptonization in the accretion channel (see Table 1, and Becker & Wolff 2007). However, it might be difficult to justify this scenario from physical point of view for observed luminosity. Indeed, effective interaction between electrons and photons is only possible if optical depth of the interaction region is appreciable ($\tau \sim 5-10$), which is unlikely at low accretion rates. Such optical depth across the accretion flow is only realized at substantially higher accretion rates corresponding to onset of accretion column (Mushtukov et al. 2015a). The optical depth along the accretion flow can be larger, however, only a small fraction of the emission emerging from polar caps follows this path due to geometric dilution.

An upper limit on the Thomson optical depth in the interaction region can be found using Eq.(18) in Mushtukov et al. (2015a): $\tau_{\rm T} \approx 0.01(\xi/0.5)^{0.5} \ll 1$. Here we adopted the GX 304−1 low-state luminosity $L_{\rm X} = 10^{34}\,{\rm erg\,s^{-1}}$, the magnetic field $B = 5\times10^{12}$ G, the NS mass $M = 1.5\,{\rm M}_\odot$ and the radius R=12 km and the ratio of the magnetospheric to the Alfvén radii $\xi = R_{\rm m}/R_{\rm A} = 0.5$. We conclude, therefore, that bulk Comptonization cannot be efficient in GX 304−1 and in other pulsars with $L_{\rm X} \leq 10^{35}\,{\rm erg\,s^{-1}}$, i.e. including X Persei.

Alternative interpretation for the hard component as thermally broadened cyclotron emission was discussed by Di Salvo et al. (1998). The expected width of such a feature corresponding to the temperature of the soft component (2–4 keV), is, however, much smaller than the observed width of the hard component. On the other hand, this scenario could still be viable if the broadening occurs in a region with higher temperature. We note that the upper layers of NS atmosphere heated by the accretion are not cooled efficiently by their thermal emission. The cooling proceeds mainly through Compton up-scattering of the low-energy photons and direct cyclotron cooling. We cannot exclude, however, that the cooling might be insufficient to prevent overheating of upper layers to $\sim 10-100$ keV as happens in non-magnetized atmospheres (Deufel et al. 2001; Suleimanov et al. 2018). In this case, thermal broadening of the cyclotron emission line, which forms in these hot layers, could be already comparable with the observed width of the hard component.

Finally, the hard component may originate from the collisionless shock above NS surface, which has been proposed for the low-luminosity states in XRPs (see e.g. Shapiro & Salpeter 1975; Langer & Rappaport 1982).[3] In this scenario, the kinetic energy of the accreting ions is assumed to transfer into their thermal energy with characteristic temperatures for ions and electrons being close to their virial temperatures. In this case, Coulomb interactions might be effective enough to transfer thermal energy of ions to the electrons which are able to cool effectively. This results in a cooling of the post-shock region, and settling of the plasma onto

[3] See also discussion in Rothschild et al. (2017) where the collisionless shock was involved to explain some observational features of XRPs at low-luminosity state.

the NS surface. The height of the post-shock region is then determined by the cooling rate and might be comparable to the NS radius (Langer & Rappaport 1982). The spectrum of the post-shock region as computed by Langer & Rappaport (1982) for $\dot{M} = 6 \times 10^{14}\,\mathrm{g\,s^{-1}}$ does qualitatively resemble the spectra observed in X Persei and GX 304−1 in the low state. The model spectra, however, were computed under assumption that plasma radiates cyclotron emission in the optically thin regime, which is not correct, therefore the calculations must be repeated with more feasible assumptions before any firm conclusions can be drawn.

4 CONCLUSION

We presented here the analysis of the spectrum of XRP GX 304−1 observed with *NuSTAR* at a very low state with $L_\mathrm{X} \sim 10^{34}\,\mathrm{erg\,s^{-1}}$. The spectrum was found to differ dramatically from the previously observed spectra of the source at higher luminosities ($L_\mathrm{X} \sim 10^{36} - 10^{37}\,\mathrm{erg\,s^{-1}}$). The latter are typical for XRPs and can be described by the single comptonized spectra in a hot electron slab with the cyclotron absorption feature at 45–60 keV. On the other hand, at a low luminosity two components with characteristic temperatures of $kT \sim 2\,\mathrm{keV}$ and $\sim 10\,\mathrm{keV}$ can be identified. A similar spectrum has been reported previously only for the persistent low-luminosity XRP X Persei. A transition between the two spectral states has, however, never been observed in any XRP.

Given the similarity in low-luminosity spectra of GX 304−1 and X Persei, it is reasonable to assume that the physical processes shaping the spectra must also be similar. The bulk Comptonization interpretation invoked previously for X Persei to explain the hard part of the spectrum is, however, problematic for GX 304−1 due to necessarily low optical depth of the accretion flow. We have also demonstrated that the two-component spectrum cannot be mimicked by the flux depression between the two components e.g. by the resonant scattering.

We thus considered two possibilities to explain the observed low-luminosity spectrum of GX 304−1. The first one is associated with potential heating of the NS atmosphere by fast ions of the accretion flow. In this case, the first, softer component is associated with a relatively deep ($\tau_\mathrm{T} > 1$) almost isothermal emission from the polar caps with a temperature $\sim 2\,\mathrm{keV}$, while the second, harder component could be connected with the cyclotron emission line which is thermally broadened in the upper overheated ($kT \geq 10 - 100\,\mathrm{keV}$) layers of the NS atmosphere. Alternatively, the observed spectrum might also emerge from the hot post-shock structure below the collisionless shock. Both of these models are purely qualitative at this stage and have to be verified by numerical modeling and comparison with the available observations of both sources.

ACKNOWLEDGEMENTS

This work was supported by the grant 14.W03.31.0021 of the Ministry of Science and Higher Education of the Russian Federation. VD thanks the Deutsches Zentrum for Luft- und Raumfahrt (DLR) and Deutsche Forschungsgemeinschaft (DFG) for financial support. VFS acknowledges the support from the DFG grant WE 1312/51-1 and from the travel grant of the German Academic Exchange Service (DAAD, project 57405000). This research was also supported by the Academy of Finland travel grant 317552 (ST, JP) and by the Netherlands Organization for Scientific Research (AAM).

REFERENCES

Becker P. A., Wolff M. T., 2007, ApJ, 654, 435
Burrows D. N., et al., 2005, Space Sci. Rev., 120, 165
Coburn W., Heindl W. A., Gruber D. E., Rothschild R. E., Staubert R., Wilms J., Kreykenbohm I., 2001, ApJ, 552, 738
Deufel B., Dullemond C. P., Spruit H. C., 2001, A&A, 377, 955
Di Salvo T., Burderi L., Robba N. R., Guainazzi M., 1998, ApJ, 509, 897
Doroshenko V., Santangelo A., Kreykenbohm I., Doroshenko R., 2012, A&A, 540, L1
Evans P. A., et al., 2009, MNRAS, 397, 1177
Farinelli R., Titarchuk L., Paizis A., Frontera F., 2008, ApJ, 680, 602
Farinelli R., Ferrigno C., Bozzo E., Becker P. A., 2016, A&A, 591, A29
Gehrels N., et al., 2004, ApJ, 611, 1005
Harrison F. A., et al., 2013, ApJ, 770, 103
Illarionov A. F., Sunyaev R. A., 1975, A&A, 39, 185
Kalberla P. M. W., Burton W. B., Hartmann D., Arnal E. M., Bajaja E., Morras R., Pöppel W. G. L., 2005, A&A, 440, 775
Klochkov D., et al., 2012, A&A, 542, L28
Kühnel M., et al., 2017, MNRAS, 471, 1553
Langer S. H., Rappaport S., 1982, ApJ, 257, 733
Lutovinov A., Tsygankov S., Chernyakova M., 2012, MNRAS, 423, 1978
McClintock J. E., Rappaport S. A., Nugent J. J., Li F. K., 1977, ApJ, 216, L15
Mushtukov A. A., Suleimanov V. F., Tsygankov S. S., Poutanen J., 2015a, MNRAS, 447, 1847
Mushtukov A. A., Tsygankov S. S., Serber A. V., Suleimanov V. F., Poutanen J., 2015b, MNRAS, 454, 2714
Priedhorsky W. C., Terrell J., 1983, ApJ, 273, 709
Reig P., 2011, Ap&SS, 332, 1
Rothschild R. E., et al., 2017, MNRAS, 466, 2752
Shapiro S. L., Salpeter E. E., 1975, ApJ, 198, 671
Suleimanov V. F., Poutanen J., Werner K., 2018, A&A, in press (arxiv:1808.10655),
Titarchuk L., 1994, ApJ, 434, 570
Treuz S., Doroshenko V., Santangelo A., Staubert R., 2018, A&A, submitted (arxiv:1806.11397),
Tsygankov S. S., Wijnands R., Lutovinov A. A., Degenaar N., Poutanen J., 2017a, MNRAS, 470, 126
Tsygankov S. S., Mushtukov A. A., Suleimanov V. F., Doroshenko V., Abolmasov P. K., Lutovinov A. A., Poutanen J., 2017b, A&A, 608, A17
Wachter K., Leach R., Kellogg E., 1979, ApJ, 230, 274
Walter R., Lutovinov A. A., Bozzo E., Tsygankov S. S., 2015, A&ARv, 23, 2
Yamamoto T., Sugizaki M., Mihara T., Nakajima M., Yamaoka K., Matsuoka M., Morii M., Makishima K., 2011, PASJ, 63, S751

This paper has been typeset from a TEX/LATEX file prepared by the author.